Nuclear-spin noise and spontaneous emission

Tycho Sleator* and Erwin L. Hahn
Department of Physics, University of California, Berkeley, California 94720

Claude Hilbert† and John Clarke
Department of Physics, University of California, Materials and Chemical Sciences Division, Lawrence Berkeley Laboratory, Berkeley, California 94720

(Received 9 March 1987)

The spontaneous emission from nuclear spins has been observed at liquid-^{4}He temperatures. The spins, ^{35}Cl nuclei, are placed in the inductor of a tuned *LCR* circuit coupled to a dc superconducting quantum interference device used as a radio-frequency amplifier. When the spins are saturated and have zero polarization, the emission is observed at the nuclear quadrupole Larmor frequency as a bump in the spectral density of the Nyquist noise current in the tuned circuit. This bump arises from the temperature-independent fluctuations in the transverse component of the nuclear magnetization. When the spins are in thermal equilibrium, on the other hand, a dip in the spectral density of the current noise is observed, arising from an induced absorption of noise power from the circuit at the Larmor frequency. The standard circuit-coupled Bloch's equation, modified to take into account radiation damping and transverse spin fluctuations, is consistent with the predictions of the Nyquist theorem and the Einstein equation for spontaneous emission. A spin-pendulum model for spin noise is described. The signal-to-noise ratio obtainable in a spin-noise measurement is discussed.

I. INTRODUCTION

The recent development[1] of the dc superconducting quantum interference device (SQUID) as a low-noise radio-frequency (rf) amplifier has made possible the detection of very weak signals at frequencies up to 300 MHz. In the present work[2] we use the SQUID as a rf amplifier to measure nuclear-spin fluctuations generated at liquid helium temperatures by a sample of spins placed in the coil of a tuned circuit. In his classic paper[3] on nuclear induction, F. Bloch noted that an ensemble of N spins of magnetic moment μ would induce in a surrounding coil very small voltages fluctuations proportional to $N^{1/2}\mu$. In our experiment, these voltage fluctuations produce current fluctuations in the tuned circuit, which are amplified by the SQUID and subsequently analyzed. In a calculation seemingly unrelated to spin fluctuations Purcell showed[4] that the spontaneous emission of radiation from an ensemble of nuclear magnetic dipoles would be enhanced if the ensemble were coupled to a resonant cavity. These two concepts have been brought together in our experiments because the current fluctuations $I_s(t)$ arising from fluctuating magnetic moments represent enhanced spontaneous emission into the circuit resistance R_i in the form of a power flow $R_i\langle I_s^2\rangle$. Nyquist noise voltages in the circuit are generated by R_i and by the spins, which are equivalent to a spin resistance R_s for frequencies at or near the Larmor frequency. The direct application of the Nyquist theorem to interpret the measured current fluctuations proves to be consistent with the use of the Einstein equation and modified Bloch equation to describe the detailed balance of the emission of spin noise power into R_i and the absorption by the spins of noise power from R_i.

At and above optical frequencies spontaneous emission from electric dipole transitions is readily detected in free space. The spontaneous emission of magnetic dipole radiation, however, is less commonly observed, although the 21-cm hyperfine line of hydrogen generated in interstellar space is well known. The spontaneous emission rate for magnetic dipole radiation is proportional to $\nu^3\mu^2$, where ν is the emitted frequency. Thus, at first sight, one hardly expects to observe spontaneous emission at radiofrequencies from a nuclear magnetic moment which is three orders of magnitude smaller than an electronic dipole moment. For a choice of $\mu=\mu_B$ (nuclear Bohr magneton) and $\nu=30$ MHz the rate is roughly 28 orders of magnitude less than that for electric dipole radiation in the visible spectrum. In fact, in free space the rate is 8×10^{-27} sec^{-1}. At wavelengths longer than optical, it is possible to couple dipole systems almost completely to cavity modes and thereby enhance the rate of spontaneous emission over that in free space. If one places the spins in a cavity with $Q=1000$, for a sample with volume $v_s=1$ cm^3 the emission rate would be enhanced by a factor of $Qc^3/2\pi\nu^3 v_s\approx10^{11}$ over the free-space value to approximately 10^{-17} sec^{-1}. At first sight, it might appear impractical to observe even this greatly enhanced emission rate. However, given that there are of the order of 10^{22} spins in the sample, by using the low-noise temperature offered by the SQUID amplifier combined with signal-averaging techniques we can observe a spontaneous emission power that is as low as 5–10 % of the Nyquist noise power generated in the same bandwidth as the spin noise.

In Sec. II we introduce the concept of spin noise and derive an expression for the fluctuations produced by an ensemble of nuclear spins. Sections III and IV describe the measurement of spin fluctuations from the ^{35}Cl nuclei

in samples of $NaClO_3$ and $KClO_3$ at the zero-field nuclear quadrupole resonance (NQR) frequency of about 30 MHz. In Sec. V we demonstrate the connection between spin noise and spontaneous emission in terms of Einstein and modified Bloch equations, and discuss the interaction between the spins and the circuit under general conditions. Section VI presents a pendulum model to account for equilibrium spin noise, while in Sec. VII we derive an expression for the signal-to-noise ratio expected from our experiments and compare it with the expression for a conventional NMR measurement. We make some concluding remarks in Sec. VIII.

II. PRINCIPLE OF SPIN NOISE: APPLICATION OF THE NYQUIST THEOREM

In the experiment, a sample of nuclear spins is placed in the inductor L_p of a tuned circuit and the spectral density of the current fluctuations is measured over the bandwidth of the circuit. The circuit resistance R_i produces a Nyquist voltage noise and therefore a current noise that, in the absence of the sample, is given by

$$S_I(\omega)=\frac{(2/\pi)k_B TR_i}{R_i^2+(\omega L_p-1/\omega C_i)^2} \tag{1}$$

for $\hbar\omega \ll k_B T$. We see that $S_I(\omega)$ is a maximum at the circuit resonant frequency $(L_p C_i)^{-1/2}$. The presence of the sample modifies the shape of this noise-power spectrum in the region of the sample resonant frequency. The influence of the sample is determined from its complex spin susceptibility[5] $\chi(\omega)=\chi'(\omega)-i\chi''(\omega)$, where χ' and χ'' are the dispersion and absorption. The complex impedance of the coil in the presence of the sample is

$$\begin{aligned} Z_p' &= i\omega L_p' = i\omega L_p[1+4\pi\xi\chi(\omega)] \\ &= i\omega[L_p+L_s(\omega)]+R_s(\omega) , \end{aligned}$$

where $\xi=v_s/v_c$ is the sample filling factor; v_s and v_c are the volume of the sample and the pick-up coil. The added spin inductance $L_s=4\pi\xi L_p\chi'$ shifts the circuit resonant frequency, while the added spin resistance $R_s=4\pi\xi\omega L_p\chi''$ modifies the damping of the circuit and acts as a source of Nyquist noise. If we assume the spins are at a temperature T_s (not necessarily equal to the bath temperature T) the spectral density of the current in the presence of the spins is given by

$$S_i(\omega)=\frac{(2/\pi)k_B[R_i T+R_s(\omega)T_s]}{(R_i+R_s)^2+[\omega(L_p+L_s)-1/\omega C_i]^2} . \tag{2}$$

Here, the term $(2/\pi)k_B R_s T_s$ is the spectral density of the Nyquist voltage noise produced by the spins and is due to fluctuations in the magnetization of the sample. In the experiment we detect the presence of the spins by their influence on the current noise in the circuit as expressed by Eq. (2).

It is useful to compute the Nyquist noise generated by the spins in terms of the microscopic parameters of the sample. Although we use a sample exhibiting nuclear quadrupole resonance (NQR) in our experiment, its response is equivalent[6] to a two-level system of spins with $I=\frac{1}{2}$ in an external magnetic field $H_z\hat{z}$. The spin density is $n=N/v_s$, where N is the total number of spins, and the Larmor frequency is $\omega_s/2\pi=\gamma H_z/2\pi$, where γ is the gyromagnetic ratio. The axis of the pickup coil is along the x direction. The magnetization along the z-axis can be expressed in terms of a spin temperature T_s:

$$M_z=(n\gamma\hbar/2)\tanh(\hbar\omega_s/2k_B T_s) . \tag{3}$$

We assume that Bloch's equations apply, and neglect departures from ideal behavior that occur in a solid, for example inhomogeneous broadening and dipolar coupling effects. Therefore,

$$\chi'(\omega)=\Delta\omega T_2\chi''(\omega) \tag{4a}$$

and

$$\chi''(\omega)=M_z\gamma T_s/2[1+(\Delta\omega)^2T_2^2] , \tag{4b}$$

where $\Delta\omega=\omega_s-\omega$, and the linewidth is given by $\Delta f_s=1/\pi T_2$. The spectral density of the Nyquist noise voltage produced by R_s is[7]

$$S_v^s(\omega)=\frac{2}{\pi}R_s\frac{\hbar\omega}{2}\coth\left[\frac{\hbar\omega}{2k_B T_s}\right] . \tag{5}$$

Combining Eqs. (3)–(5) and neglecting terms of order $\Delta\omega/\omega_s \ll 1$, we obtain

$$S_v^2(\omega)=\frac{\xi L_p\omega_s^2 n\gamma^2\hbar^2 T_2}{1+(\Delta\omega)^2T_2^2} . \tag{6}$$

Remarkably, because of the cancellation of the hyperbolic terms in Eqs. (3) and (5), $S_v^s(\omega)$ is independent of temperature throughout both the quantum ($\hbar\omega \gg k_B T_s$) and classical ($\hbar\omega \ll k_B T_s$) regimes.

It is also of interest to compute the mean square voltage noise generated by the spins,

$$\langle V_s^2\rangle=\int_{-\infty}^{\infty}S_v^s(\omega)d\omega=\pi\xi L_p\omega_s^2 n\gamma^2\hbar^2 . \tag{7}$$

Note that $\langle V_s^2\rangle$ is independent of the linewidth Δf_s of the transition.

We can understand both the temperature independence of S_v^s and the linewidth independence of $\langle V_s^2\rangle$ from a different point of view by applying Faraday's law of induction to obtain the mean-square voltage $\langle V_s^2\rangle=4\pi\xi L_p\omega_s^2 v_s\langle M_x^2\rangle$ in terms of the mean-square magnetization $\langle M_x^2\rangle$. For a sample with N spins

$$\langle M_x^2\rangle=N\langle\mu_x^2\rangle/v_s^2=n\gamma^2\hbar^2\langle I_x^2\rangle/v_s , \tag{8}$$

where the magnetic moment of a single spin is $\mu_x=\gamma\hbar I_x$ and $\langle I_x^2\rangle=\frac{1}{4}$ for spin $I=\frac{1}{2}$. Making these substitutions in the expression for Faraday's law, we recover Eq. (7). This derivation is essentially equivalent to Bloch's argument discussed in the Introduction.

We note here that the temperature independence of spin fluctuations holds only for a two-level ($I=\frac{1}{2}$) system. To compute the spectral density for arbitrary spin with equally spaced levels, the expression for M_z in Eq. (3) must be replaced by

$$M_z = n\gamma\hbar\left[\frac{2I+1}{2}\coth\left[\frac{(2I+1)\hbar\omega_s}{2k_BT_s}\right] - \tfrac{1}{2}\coth\left[\frac{\hbar\omega_s}{2k_BT_s}\right]\right]$$

$$= n\gamma\hbar I B_I(x) , \tag{9}$$

where $B_I(x)$ is the Brillouin function for spin I and $x \equiv \hbar\omega_s I/k_BT_s$. The voltage noise produced by the sample becomes

$$\langle V_s^2\rangle = 2\pi\xi L_p\omega_s^2 n\gamma^2\hbar^2 I B_I(x)\coth(\hbar\omega_s/k_BT_s)$$

$$= \langle V_s^2\rangle_{I=1/2} 2I B_I(x)\coth(\hbar\omega_s/k_BT_s) . \tag{10}$$

In the high-temperature limit ($\hbar\omega_s I \ll k_BT_s$) we find

$$\langle V_s^2\rangle = (\tfrac{4}{3})I(I+1)\langle V_s^2\rangle_{I=1/2} ,$$

while in the low-temperature limit ($\hbar\omega_s \gg k_BT_s$),

$$\langle V_s^2\rangle = 2I\langle V_s^2\rangle_{I=1/2} .$$

Thus, for $I > \frac{1}{2}$, the voltage fluctuations $\langle V_s^2\rangle$ (or S_v^s) do depend on temperature in the region $\hbar\omega_s \sim k_BT_s$, but become independent of temperature in the high- and low-temperature limits. The significance of the temperature independences of S_v^s for our experiment will be discussed later in the paper.

III. EXPERIMENTAL PROCEDURES

The configuration of the experiment, which is carried out at liquid-helium temperatures, is shown in Fig. 1.

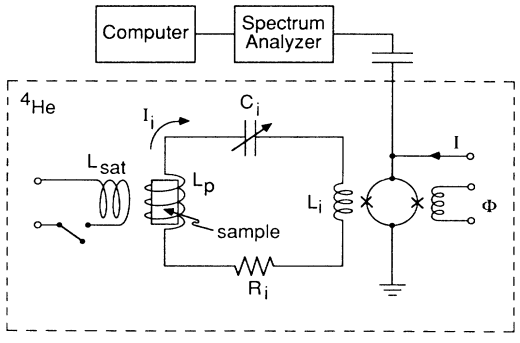

FIG. 1. Experimental configuration. Components in dashed box are immersed in liquid ^{4}He.

The sample of nuclear spins is contained in a superconducting coil L_p in series with a capacitor C_i. A superconducting inductance L_i ($\ll L_p$), also in series, represents the input coil of a dc SQUID. The capacitance C_i consists of a fixed silver-mica capacitor in parallel with a Murata-Erie MVM020W air capacitor, which can be adjusted from the top of the cryostat. The whole circuit is superconducting with the exception of the capacitors; the resistance R_i represents losses in the capacitors and contact resistance. An additional coil $L_{\rm sat}$, wound around the sample and the pickup coil, is used to apply continuous or pulsed rf signals to the sample to saturate the spins or test the system. This coil is wound perpendicularly to L_p and is opened during data acquisition to eliminate the possibility of external noise injection. A current I_i in the input circuit generates a magnetic flux Φ_i in the SQUID loop L, producing an output voltage V across the SQUID. The dc SQUID is a flux-to-voltage transducer which is linear for small signals ($\Phi \ll \Phi_0 \equiv h/2e$). Our SQUID's are planar thin-film devices[1] fabricated with standard photolithographic methods, and tightly coupled to a four-turn planar superconducting input coil. They can be operated[1] at frequencies up to 300 MHz with a typical power gain of 20 dB. The noise temperature T_N (referred to the input circuit) for a particular device was measured to be 1.7 ± 0.5 K at 100 MHz at an operating temperature of 4.2 K. The noise temperature scales with the bath temperature and the signal frequency so that for our experiment, which involves measurements at 30 MHz and 1.5 K, the SQUID noise temperature T_N is reduced to 0.2 K.

Like any other amplifier, however, a dc SQUID has a back action on the input circuit. The SQUID is coupled to the input circuit predominantly by the mutual inductance M_i between the SQUID loop L and the input coil L_i, and to a small extent by the parasitic capacitance C_p between these two coils. A fraction of the SQUID current noise couples inductively into the input circuit, but this contribution to the noise in the input circuit is less than 10% of the Nyquist noise of the input resistor under our experimental conditions. The SQUID inductance also partially screens the input coil L_i, but since $L_p \sim 10^3 L_i$ this effect can be neglected. On the other hand, for the high values of Q used here, capacitive feedback can change the input impedance substantially. The feedback effectively adds a resistance ΔR_i to the input circuit, the sign and magnitude of which depend on the SQUID bias conditions.[1] Fortunately, the SQUID output noise coupled into the input circuit via this parasitic capacitance is negligible for our SQUID amplifiers, so that ΔR_i can be considered to be noiseless for the rest of this paper. The presence of the SQUID modifies the spectral density of the current fluctuations in the input circuit given by Eq. (2) to give

TABLE I. Properties of $NaClO_3$ and $KClO_3$.

Sample	f_s (MHz)	Δf_s (kHz)	T_2 (μs)
$NaClO_3$	30.6859	1.3	240
$KCl)_3$	29.0389	0.64	500

$$S_I(\omega)=\frac{(2/\pi)k_B[R_iT+R_s(\omega)T_s]}{[R_i+R_s(\omega)+\Delta R_i]^2+\{\omega[L_i+L_p+L_s(\omega)]-1/\omega C_i\}^2}\ , \tag{11}$$

where we have ignored the effect of the SQUID noise coupled back inductively into the input circuit.

The dc SQUID has an output impedance of about 10 Ω which is matched to a low-noise room-temperature amplifier with a 50-Ω-input impedance via a cryogenic stainless-steel coaxial cable and a capacitor. The amplified SQUID output is connected to an HP3835 spectrum analyzer interfaced to an HP9816 computer for data storage, averaging, and analysis. The noise temperature of the amplifier is about 100 K, provided its input is optimally matched to the SQUID output. Since the SQUID power gain is typically 20 dB, the amplifier noise is equivalent to a noise temperature of about 1 K referred to the SQUID input circuit, compared to a bath temperature of 1.5 K and a SQUID noise temperature of 0.2 K. Hence the SQUID and the following amplifier contribute about 1.2 K of noise, that is, at the resonant frequency they produce roughly half of the total noise output.

Noise measurements were made separately on two different powdered samples, $NaClO_3$ and $KClO_3$. For $NaClO_3$ the sample volume was 0.63 cm^3 resulting in a total number of spins N of 6×10^{21}, and the filling factor ξ was about 0.35. The ^{35}Cl nucleus has spin $I=\frac{3}{2}$ and is split by the nuclear (electric) quadrupole interaction into two doubly degenerate energy levels corresponding to $I_z=\pm\frac{3}{2}$ and $I_z=\pm\frac{1}{2}$. The transition frequencies ($\omega_s/2\pi$), linewidths (Δf_s), and transverse relaxation times ($T_2=1/\pi\Delta f_s$), measured at 1.5 K in separate pulsed experiments, are given in Table I.

IV. EXPERIMENTAL RESULTS

We performed two separate experiments corresponding to two different values of T_s in Eq. (2).

A. Thermal equilibrium

In the first experiment, the spins were allowed to reach equilibrium ($T_s=T$) with the helium bath at 1.5 K. Before the experiment could be performed, however, we had to shorten the enormously long spin-lattice relaxation time T_1 of the sample (days). By exposing the sample to 10^6 Rad of 1.0-Mev γ rays from a ^{60}Co source, we reduced T_1 to about 20 min at 1.5 K. In the high-temperature limit $\hbar\omega \ll k_BT$, the spectral density of the current noise in the input circuit is given by

$$S_I(\omega)\,|_{\,T_s=T}=\frac{(2/\pi)k_BT[R_i+R_s(\omega)]}{[R_i+\Delta R_i+R_s(\omega)]^2+|X|^2}\ , \tag{12}$$

where $X\equiv j\omega[L_p+L_i+L_s(\omega)]-j/\omega C_i$. We obtain a simple form for S_I when the circuit is tuned exactly to the Larmor frequency $\{\omega_s=[(L_p+L_i)C_i]^{-1/2}\}$. If we assume Δf_s is much less than the circuit bandwidth and ignore $\Delta R_i \ll R_i+R_s$, at or near resonance $X\simeq0$ and Eq. (12) reduces approximately to $2k_BT/\pi(R_i+R_s)$. Under these conditions the spins produce a "dip" in the spectral density as ω is scanned through the NQR frequency and $R_s(\omega)$ passes through a maximum, as illustrated in Fig. 2. These data were taken over a period of 3 h with the resolution bandwidth of the spectrum analyzer set to 300 Hz. The dip is largest at the ^{35}Cl NQR frequency (indicated by an arrow) measured separately. Furthermore, by fitting the data to Eq. (12) we find good agreement with the parameters ω_s and T_2 listed in Table I. For the data in Fig. 2 the fit also yields a value of $\Delta R_i\approx-0.5R_i$.

Strictly speaking, the system is not in thermal equilibrium for $\Delta R_i\neq0$. If we write the total resistance of the circuit as $R_i'+R_s$, where $R_i'=R_i+\Delta R_i$, Eq. (12) becomes

$$S_I(\omega)\,|_{\,T_s=T}=\frac{(2/\pi)k_BT[R_i'+R_s(\omega)]\{1-\Delta R_i/[R_i'+R_s(\omega)]\}}{[R_i'+R_s(\omega)]^2+|X|^2}\ , \tag{12a}$$

so that the effective temperature is $T\{1-\Delta R_i/[R_i'+R_s(\omega)]\}$. The term $(-2/\pi)k_BT\Delta R_i$ represents an additional source term and for $\Delta R_i<0$ is equivalent to the injection of additional noise into the circuit. In addition, ΔR influences the Q $[=\omega(L_i+L_p)/(R_i+\Delta R_i)]$ of the circuit. For the data in Fig. 2, Q is enhanced by a factor of 2 over its value in the absence of the SQUID. It is useful to define the intrinsic quality factor $Q_0=\omega(L_i+L_p)/R_i$ in the absence of the sample and of the loading by the SQUID. We measure Q_0 by turning off the SQUID bias current and measuring the ring-down time of the tuned circuit following an applied rf pulse; even with the SQUID turned off there is sufficient reactive coupling to produce a signal from the post amplifier. The data yield the values $Q=7320$, $R_s(\omega_s)/R_i'=0.12$, and $R_s(\omega_s)/R_i'Q=4\pi\xi\chi''(\omega_s)=1.6\times10^{-5}$. The dotted line in Fig. 2 indicates the response we would expect from this fit

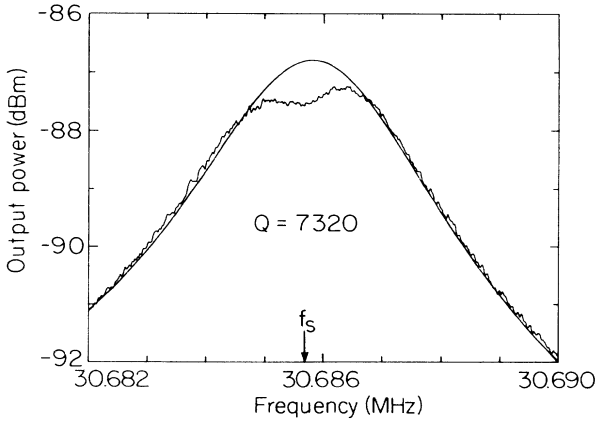

FIG. 2. Spectral density of noise current for a $NaClO_3$ sample in thermal equilibrium at 1.5 K; ω_s is at circuit resonance frequency.

in the absence of the sample (but in the presence of the SQUID).

Figure 3 shows data for the same sample in the case where the circuit is not exactly tuned to the Larmor frequency. We observe a peak below ω_s and a dip above ω_s due to the influence of both the spin resistance and spin inductance. In this case a fit reveals that $\Delta R_i = -0.04 R_i$, so that the spins and bath were very nearly in equilibrium.

B. Saturated spins: Spin noise

In the second experiment, the ^{35}Cl spins of a sample of $NaClO_3$ with an extremely long T_1 (days) were saturated by applying continuous rf excitation at resonance by means of the coil L_{sat}. After the excitation was turned off (and the coil L_{sat} opened) we measured the spectral density over a time much less than T_1. A saturated sample has zero-spin population difference, so that $M_z = \chi = R_s = L_s = 0$ and $T_s = \infty$. According to Eq. (6), however, the voltage noise produced by R_s ($\propto R_s T_s$ for $\hbar\omega \ll k_B T$) is independent of T_s for a given frequency. The spectral density of the current becomes

$$S_i(\omega)\,|_{T_s=\infty} = \frac{(2/\pi)k_B[R_i T + R_s(\omega)T_s]}{[R_i + \Delta R_i]^2 + [\omega(L_p + L_i) - 1/\omega C_i]^2} \,. \tag{13}$$

Thus, one would expect to observe a "bump" in the spectral response arising from the term $R_s T_s$ in the numerator of Eq. (13).

An example of our data for a sample of $NaClO_3$, which was obtained in a resolution bandwidth of 300 Hz averaged for 7 h, is shown in Fig. 4(a); the NQR frequency is indicated with an arrow. From the fit of the data to Eq. (13) we find $Q = 3430$ and $R_s(\omega_s)T_s/R_i T = 0.06$. A measurement with the SQUID turned off yielded $Q_0 = 4000$ so that $4\pi\xi\chi''(\omega_s) = R_s(\omega_s)T_s/R_i T Q_0 = 1.4\times 10^{-5}$, a value

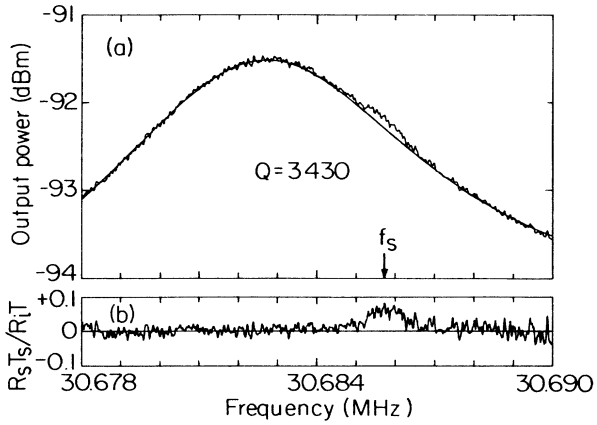

FIG. 4. Spectral density of (a) noise current for a $NaClO_3$ sample with saturated spins ($T_s = \infty$), and (b) nuclear spin noise of $NaClO_3$ sample obtained from (a).

in good agreement with that obtained in the previous (equilibrium) case. The dotted line indicates the expected power spectrum in the absence of the sample. By comparing this expected power spectrum to the data using Eq. (13) the excess noise due to the spins $[T_s R_s(\omega)]$ can be determined and is shown in Fig. 4(b).

Figure 5 shows data from a similar experiment performed on a sample of $KClO_3$, obtained by averaging for 2.3 h with a bandwidth of 300 Hz. As expected, for a given Q the bump produced by $KClO_3$ is both narrower and higher than that of $NaClO_3$. Since the area of the bump $[\int T_s R_s(\omega)d\omega]$ is independent of the linewidth, the narrow linewidth of $KClO_3$ compared with $NaClO_3$ leads to a higher bump. When the data are fitted to Eq. (11), we find $R_s(\omega_s)T_s/R_i T = 0.103$ which, for the measured value of $Q_0 = 4000$, gives $4\pi\xi\chi''(\omega_s) = 2.6\times 10^{-5}$.

We conclude this experimental section with two comments. First, one could extend these spin-noise experi-

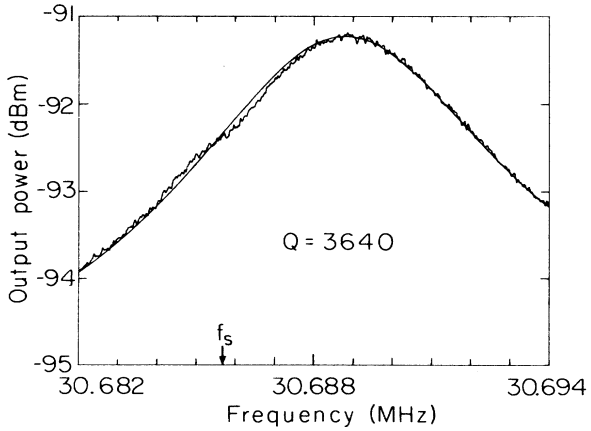

FIG. 3. Spectral density of noise current for a $NaClO_3$ sample in thermal equilibrium at 1.5 K; ω_s is below circuit resonance frequency.

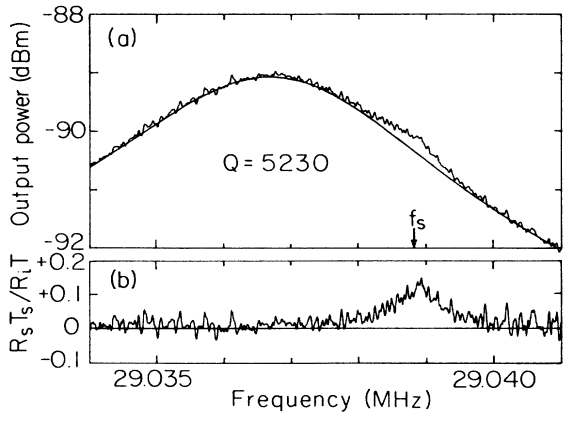

FIG. 5. Spectral density of (a) noise current for a $KClO_3$ sample with saturated spins ($T_s = \infty$), and (b) nuclear spin noise of $KClO_3$ sample obtained from (a)

ments by inverting the equilibrium magnetization M_z to $-M_z$ with a 180° pulse. In the limit $R_s \ll R_i$ the magnitude of the noise bump is expected to be three times greater than that observed for $M_z = 0$. As $R_s \to R_i$, the noise bump approaches a singularity. If the threshold condition $R_s \gtrsim R_i$ could be achieved, maser[8] oscillations would result. Second, the value of T_1 does not enter into either experiment except to determine the rate at which the sample reaches thermal equilibrium. If one were to introduce a pickup coil with its axis parallel to the direction of spin polarization, the longitudinal relaxation process would induce into the coil exceedingly small voltage fluctuations about zero frequency. In practice, it appears that these fluctuations would be too small to be detected.

V. BLOCH-EINSTEIN POWER EQUATION

The relationship between spin fluctuations and spontaneous emission can be understood by examining the average noise power flow ΔP between the spins and circuit. In this section we derive an expression for the power flow between the spins and the resistor R_i. The equivalence of this expression to the Einstein equation for detailed balance and to the predictions of the Bloch equations coupled to the circuit is demonstrated.

A. Circuit description of the power flow

In a circuit with a resistor R_s at temperature T_s and a resistor R_i at temperature T the net power from R_s into R_i is

$$\Delta P = \int_{-\infty}^{\infty} \frac{\hbar\omega R_s R_i [\coth(\hbar\omega/2k_B T_s) - \coth(\hbar\omega/2k_B T)]}{\pi[(R_i+R_s)^2+(X_i+X_s)^2]} d\omega \ , \tag{14}$$

where $X_i = \omega L_p - 1/\omega C_i$ and $X_s = \omega L_s$. The equivalence of Eq. (14) to the Einstein equation of detailed balance will be demonstrated in the case $\Delta\omega_s \ll \Delta\omega_c$, $\omega_s = \omega_c$, $\Delta\omega_c \ll \omega_c$, and $R_s \ll R_i$. Equation (14) becomes

$$\Delta P = P_s - P_R$$

$$= \frac{\langle V_s^2 \rangle}{R_i} - \frac{\hbar\omega_s}{R_i \pi} \coth\left[\frac{\hbar\omega_s}{2k_B T}\right] \int_{-\infty}^{\infty} R_s(\omega) d\omega \ , \tag{15}$$

where $\langle V_s^2 \rangle$ is given by Eq. (7) and we have used the fact that $\Delta\omega_s \ll \omega_s$ to remove $\omega \coth(\hbar\omega/2k_B T)$ as a constant from the integral. The term $\langle V_s^2 \rangle / R_i$ in Eq. (15) is the emitted spin noise power P_s absorbed by the resistance R_i, while the integral is the power P_R absorbed by the spins due to the Nyquist noise generated by the resistor R_i. Using Eq. (7) and $Q = \omega_s L_p / R_i$ (valid for $L_i \ll L_p$), we find[9]

$$P_s = \langle V_s^2 \rangle / R_i = \pi Q \omega_s N \gamma^2 \hbar^2 / v_c \ . \tag{16}$$

In Eq. (15), $R_s = 4\pi\xi\omega L_p \chi''$, where χ'' is given by Eq. (4b), and $M_z = \gamma\hbar\Delta N / 2v_s$, where $\Delta N = N_\uparrow - N_\downarrow$ is the total population difference between ground and excited states. The power absorbed by the spins is therefore

$$P_R = [\pi Q \omega_s \gamma^2 \hbar^2 \Delta N \coth(\hbar\omega_s / 2k_B T)] / v_c \ . \tag{17}$$

Using Eqs. (16) and (17) we can convert Eq. (15) to the familiar form of Einstein's detailed balance equation,

$$\Delta P = \frac{\hbar\omega_s}{2} A \left[N - \Delta N(T_s) \coth\left[\frac{\hbar\omega_s}{2k_B T}\right] \right] \tag{18}$$

$$= \hbar\omega_s A \left[N_\downarrow(T_s) - \frac{\Delta N(T_s)}{e^{\hbar\omega_s / k_B T} - 1} \right] . \tag{18a}$$

The rate of spin spontaneous emission into the resonant cavity is given by $A = 2\pi Q \hbar \gamma^2 / v_c$, a result which can be derived independently by applying Fermi's golden rule for absorption of radiation by the spins, and by specifying the density of states for a single cavity mode[4] to be $\mathcal{D}_c(\omega_s) = 2Q/\pi\omega_s v_c$. The equivalence of Eqs. (15) and (18) demonstrates the close connection between spin fluctuations and spontaneous emission and shows that the bump observed in Figs. 4 and 5 represents spontaneous emission from the spins into the circuit.

The spin noise power $P_s = (\hbar\omega_s/2) AN$ [Eq. (16)] obtained from the temperature-independent term in the Nyquist formula is identical with the spontaneous emission power [Eq. (18a)] only in the limit $\hbar\omega_s \ll k_B T_s$ and $N_\downarrow \approx N/2$. However, ΔP conforms to the Nyquist prediction Eq. (15) for all spin temperatures T_s.

These data indicate that the spontaneous emission rate for one spin is extremely low. The rate $A \approx 8 \times 10^{-17}$ sec^{-1} (about one spin flip in 10^8 years), corresponds to a total emissive power $P_s = 5 \times 10^{-21}$ W from $N = 6 \times 10^{21}$ spins. This power is about 5% of the Nyquist noise power $4k_B T/\pi T_2 = 10^{-19}$ W generated in the bandwidth of the spin noise $1/\pi T_2$.

B. Analysis of power flow with the Bloch equation

We now present an evaluation of the flow of power ΔP, valid for arbitrary values of R_i and R_s, in terms of Bloch's equations modified to include the effect of the circuit. The analysis is confined to the case of a homogeneously broadened two-level system. Our treatment of the case of spin noise will require an additional noise term in Bloch's equations to account for the fluctuating magnetization. Before discussing the case of spin noise, however, we consider the response of the system to an applied coherent field $H_x(t) = 2H_1(t)\cos\omega_f t$, where $H_1(t)$ is the component rotating at a frequency $\omega_f/2\pi$. In a frame of reference rotating at this frequency, Bloch's equations are given by

$$\frac{dm(t)}{dt} + \left[\frac{1}{T_2} - i\Delta\omega_f\right] m = -i\gamma M_2 H(t) \ , \tag{19}$$

and

$$\frac{dM_z(t)}{dt} = -\gamma \,\mathrm{Im}[m^*(t)H(t)] - \frac{M_z(t)-M_0}{T_1} \ , \quad (20)$$

where $m(t)=u(t)-iv(t)$ is the transverse magnetization in the rotating frame, $\Delta\omega_f=\omega_s-\omega_f$, and Im is the imaginary component. The total field $H(t)$ is the sum of two contributions $H(t)=H_1(t)+H_r(t)$, where $H_1(t)$ is the externally applied field. The response field $H_r(t)$ accounts for the coupling of the spins to the circuit. If the circuit Q is sufficiently small (a precise definition of the low Q limit is given in Appendix A) the circuit responds to the voltage induced by the spins with negligible delay. As shown in Appendix A, the response field can then be written as $H_r(t)=-ik(\Delta\omega_{sc})m(t)$, where $\Delta\omega_{sc}=\omega_s-\omega_c$, and $k(\Delta\omega_{sc})=k'(\Delta\omega_{sc})-ik''(\Delta\omega_{sc})$ is a complex coupling constant with $\omega_c=(LC)^{-1/2}$. Previous treatments[10,11] of radiation damping in NMR, which employ the low-Q-limit condition $\omega_s/2Q \gg 1/\tau_R$ at resonance ($\Delta\omega_{sc}=0$), yield $k'(0)=2\pi Q\xi$ and $k''(0)=0$, where $1/\tau_R=\gamma M_z k'(0)$ is the radiation damping rate. In terms of the applied field H_1, Bloch's equations in the low-Q limit for $\Delta\omega_{sc}\neq 0$ are written as

$$\frac{dm(t)}{dt} + \left[\frac{1}{T_2'} - i\Delta\omega_f'\right] m = -1\gamma M_z H_1(t) \quad (21a)$$

and

$$\frac{dM_z(t)}{dt} = -\gamma \,\mathrm{Im}[m^*(t)H_1(t)] + \gamma |m|^2 k' - \frac{M_z(t)-M_0}{T_1} , \quad (21b)$$

where

$$1/T_2' = 1/T_2 + \gamma k' M_z \quad (22a)$$

and

$$\Delta\omega_f' = \Delta\omega_f + \gamma k'' M_z \ . \quad (22b)$$

The term $\gamma k' |m(t)|^2 = \gamma k'[u^2(t)+v^2(t)]$ represents the effect of coherent emission, which shortens T_2 to the value T_2' through the process of radiation damping [or more appropriately, by coherent response to the radiation reaction field $H_r(t)$]. In addition, the Larmor frequency ω_s is apparently shifted to the value $\omega_s'=\omega_s+\gamma k'' M_z$ (frequency pulling). Note that these effects of radiation damping will not be observed,[11] according to Eqs. (19) and (20), when the spin susceptibility $\chi=m/H(t)$ is measured with respect to the total field $H(t)$. When the low Q condition is violated, we cannot assume that $H_r(t)=-ikm$. Instead $H_r(t)$ must be described [see Appendix A, Eq. (A4)] in terms of the convolution

$$H_r(t) = -ik(t)*m(t) = -i(2\pi)^{-1/2}\int_0^\infty k(\tau)m(t-\tau)d\tau \ .$$

The coupling coefficient

$$k(t) = (2\pi)^{-1/2}\int_{-\infty}^{\infty} k(\omega)e^{-i\Delta\omega t}d(\Delta\omega)$$

is the Fourier transform of

$$k(\omega) = 2\pi\xi Q R_i / Z_c(\omega) \ , \quad (23)$$

where $Z_c=R_i[1+i(2Q/\omega)(\omega-\omega_c)]$ is the impedance of the circuit in the absence of spins.

We now adapt the Bloch Eqs. (19) and (20) to the case of spin noise. The fields $H_1(t)$ and $H_r(t)$ are defined as random noise fields, which are no longer coherent at a single frequency. For convenience we choose the frame of reference to be at the Larmor frequency [$\Delta\omega_f=0$ in Eq. (19)]. Also, additional terms must be added to the Bloch Eqs. (19) and (20) to account for the fluctuating transverse magnetization. To do this we assume the total magnetization $m(t)$ is the sum of two terms $m(t)=m_r(t)+m_s(t)$, where m_r is the "response" magnetization which obeys Eq. (19), while $m_s(t)$ plays the role of a noise source term. The Bloch equations modified to include spin noise are therefore

$$\frac{dm_r(t)}{dt} + \frac{1}{T_2} m_r(t) = -i\gamma M_z H(t) \ , \quad (24a)$$

$$\frac{dM_z(t)}{dt} = -\gamma \,\mathrm{Im}\{[m_r^*(t)+m_s^*(t)]H(t)\} - \frac{M_z(t)-M_0}{T_1} \ , \quad (24b)$$

$$H(t) = H_1(t) - ik(t)*[m_r(t)+m_s(t)] \ , \quad (24c)$$

with the convolution $ik(t)*[m_r(t)+m_s(t)]$ expressed by Eq. (A4) in Appendix A. Equations (24a) and (24b) form a set of coupled Langevin equations with two source terms, H_1 and m_s. The field H_1 arises from fluctuations in the resistor R_i while m_s arises from the spins. The remaining quantities H, m_r, dM_z/dt can be expressed in terms of H_1 and m_s. The magnetization m_r is nonzero only when the susceptibility is nonzero at finite spin temperature T_s, whereas m_s is temperature independent and does not obey the Bloch equations. We emphasize that the way m_s appears in Eqs. (24) is only postulated and the validity of Eqs. (24) can be justified only by the accuracy of their predictions.

To solve Eqs. (24) we assume that the time average of terms in Eq. (24b), coupled to Eq. (24a), allows M_z to be fixed at a spin temperature T_s because T_1 is very long compared to the time in which spin noise measurements are made. Our goal is to compute the power flow from the spins into the circuit, $\Delta P = H_0 v_s \langle dM_z/dt \rangle_c$, where the brackets indicate the time average due only to the effect of the circuit. Therefore the spin-lattice relaxation term is dropped because it accounts for unobserved power flow between spins and lattice. The Fourier transforms of Eqs. (24a) and (24c) yield

$$m_r(\Delta\omega) = 2\chi H(\Delta\omega) \quad (25)$$

and

$$H(\Delta\omega) = H_1(\Delta\omega) - ik(\omega)[m_r(\Delta\omega)+m_s(\Delta\omega)] \ . \quad (26)$$

We use Eq. (24b), dropping the term T_1 as explained above, to find

$$\Delta P=\lim_{T_0\to\infty}\frac{1}{2T_0}\int_{-T_0}^{T_0}-v_s\omega_s\,\mathrm{Im}\{[m_r^*(t)+m_s^*(t)]H(t)\}dt$$
$$=\lim_{T_0\to\infty}\frac{1}{T_0}\int_{-\infty}^{\infty}-v_s\omega_s\,\mathrm{Im}\{[m_r^*(\Delta\omega)+m_s^*(\Delta\omega)]\times H(\Delta\omega)\}d\Delta\omega \quad (27)$$

over a time ($T_0\to\infty$) average. To express Eq. (27) in terms of the source terms m_s and H_1, we rewrite m_r as

$$m_r=2\chi(H_1-ikm_r-ikm_s)$$
$$=(2\chi H_1-i2\chi km_s)/(1+i2\chi k)$$
$$=(Z_c/Z_t)2\chi H_1-(Z_s/Z_t)m_s\ , \quad (28)$$

where $Z_s=i4\pi\chi QR_i$ is the impedance of the spins and $Z_t=Z_c+Z_s$ is the total circuit impedance. We have used the relation $i2k\chi=Z_s/Z_c$, where k is given by Eq. (23). Combining Eqs. (26), (27), and (28) we find

$$\Delta P=\lim_{T_0\to\infty}\frac{1}{T_0}\int_{-\infty}^{\infty}|Z_c/Z_t|^2[-v_s\omega_s^2\chi''|H_1(\Delta\omega)|^2+v_s\omega_s k'|m_s(\Delta\omega)|^2]d\Delta\omega$$
$$=\int_{-\infty}^{\infty}|Z_c/Z_t|^2[-v_s\omega_s 2\chi''S_{H_1}(\Delta\omega)+v_s\omega_s k'S_{ms}(\Delta\omega)]d\Delta\omega\ . \quad (29)$$

The spectral density of the field H_1 is S_{H_1}, and S_{m_s} is the spectral density of the fluctuations in the transverse magnetization m_s. We compute S_{H_1} by finding the spectral density $S_{H_x}(\omega)=S_{H_1}(\Delta\omega)/2$ of the magnetic field in the laboratory frame $H_x(t)=2H_1(t)\cos\omega_s t$:

$$\frac{S_{H_x}(\omega)}{8\pi}=\mathcal{D}_c(\omega)\frac{\hbar\omega}{4}\coth\left[\frac{\hbar\omega}{2k_BT}\right].$$

This is a spectral density which is defined from the noise source R_i as though the spins were absent. The density of states is given by $\mathcal{D}_c(\omega)=(2Q/\omega\pi v_c)|R_i/Z_c(\omega)|^2$ in which the restriction $\omega_s=\omega_c$ is removed. We can obtain an expression for $S_{m_s}(\omega)$ by setting $\Delta P=0$ in Eq. (29) for $T_s=T$. It is found that

$$S_{m_s}=(n\gamma^2\hbar^2/2v_s)[T_2/\pi(1+\Delta\omega^2T_2^2)]$$

as expected, where the factor of $\gamma^2\hbar^2/2v_s$ is the spectral density of the spins. By substituting these expressions for S_{H_1} and S_{m_s} into Eq. (29) we find that Eq. (29) is equivalent to the Nyquist formula [Eq. (14)]. This equivalence supports the conclusion that Eqs. (24) represent the correct modification to Bloch's equations when spin noise is taken into account.

The first term in the integrand of Eq. (29) represents the absorption by the spins of the magnetic field energy produced by noise from R_i at temperature T. The second term represents emission of noise power from the spins as a result of radiation damping caused by the noise field $-ik'm_s$ [Eq. (24c)] emitted into the circuit. After the second term is integrated over frequency ω in the limit $R_s/R_i\ll 1$, it becomes equivalent to the term $\hbar\omega_s AN/2$ in Eq. (17) and leads to the interpretation that spontaneous emission of the spin system is accounted for by the mechanism of radiation damping.

Physically the spins couple with the entire cavity noise field $H(t)$ given by Eq. (24c), while Eq. (29) indicates the spin absorption of only the noise field $H_1(t)$ produced by R_i. The Nyquist relation [Eq. (2)] shows that for $R_i=0$ a fluctuating noise current remains in the circuit. This current corresponds to a spin noise field $-ik'm_s$ which is simultaneously emitted and absorbed by the spins as they couple to the single cavity mode. The spin noise field is modified by any circuit impedance, and is taken into account by adding and subtracting the term $2v_s\omega_s\chi''|k|^2|m_s|^2$ to the right-hand side of Eq. (29). The spectral field noise from both R_i and the spins is given by $|H_n(\Delta\omega)|^2=|H_1(\Delta\omega)|^2+|k'|^2|m_s(\Delta\omega)|^2$, which becomes the total noise in the absence of spin absorption ($\chi=0$, $|Z_c/Z_t|=1$). From the expression for $H(\Delta\omega)$ [Eq. (26)] and the relation $m_r=2\chi H(\Delta\omega)$, it follows that $|H(\Delta\omega)|^2=|H_n(\Delta\omega)|^2|Z_c/Z_t|^2$. From the combination of these relations the expression for ΔP in terms of the total field intensity $|H(\Delta\omega)|^2$ becomes

$$\Delta P=\lim_{T_0\to\infty}\frac{1}{T_0}\int_{-\infty}^{\infty}[-v_s\omega_s 2\chi''|H(\Delta\omega)|^2+v_s\omega_s k_T|m_s(\Delta\omega)|^2]d\Delta\omega\ ,$$

where $k_T=2\pi\omega L\xi(R_i+R_s)/|Z_t|^2$.

VI. SPIN NOISE PENDULUM MODEL

A pendulum model of the Bloch magnetization M_0 coupled to a circuit (see Appendix B) provides further insight into the connection between radiation damping and fluctuating spin magnetization. Suppose a coherent pulse H_1 tips $M(T_s)$ through an angle θ from the initial equilibrium value at spin temperature T_s. After the pulse H_1 is removed the longitudinal and transverse magnetizations are given by $M_z=M\cos\theta$ and $|m|=M\sin\theta$, where we have defined $M=(|m|^2+M_z^2)^{1/2}$ as the magnitude of the total magnetization vector. The coherent power radiated is obtained from Eq. (20) in the limit $T_1,T_2\to\infty$. Using $H(t)=k'M\sin\theta$ with $k'=2\pi Q\xi$, we find

$$P_s^{\mathrm{coh}}=\omega_s kM^2\sin^2\theta=2\pi\xi v_s Q\omega_s M^2\sin^2\theta$$
$$=H_0v_sM\theta^2/\tau_r\quad(\theta\ll 1)\ . \quad (30)$$

The coherent radiation damping rate is well known[10,11] to be $1/\tau_r = 2\pi\xi M\gamma Q$ in the low Q limit where $1/\tau_r \ll \omega/2Q$. The stored magnetic energy gained by the spins after the pulse is given by

$$E = H_0 v_s M(1-\cos\theta) = H_0 v_s M\theta^2/2 \quad (\theta \ll 1) . \tag{31}$$

Thus, for $\theta \ll 1$, the radiated power can be expressed in terms of the stored magnetic energy as

$$P_s^{\rm coh} = 2E/\tau_r . \tag{32}$$

In the incoherent case appropriate for spin noise we find that Eqs. (30), (31), and (32) remain valid for $R_s \ll R_i$ if θ^2 is replaced with $\langle\theta^2\rangle$, where

$$\langle\theta^2\rangle = \frac{\langle M_x^2\rangle + \langle M_y^2\rangle}{M^2} = \frac{2\langle M_x^2\rangle}{M^2} = \frac{N\gamma^2\hbar^2}{2M^2 v_s} \tag{33}$$

is the mean-square tipping angle of the spins. Equation (33) when combined with Eq. (30) yields Eq. (16). In addition, when Eq. (33) is combined with Eq. (31) we find

$$E = (\hbar\omega_s/2)\coth(\hbar\omega_s/2k_BT_s) = k_BT_s \quad (k_BT_s \gg \hbar\omega_s) \tag{34}$$

and $P_s^{\rm incoh} = 2k_BT_s/\tau_r$ is the incoherent radiated power by analogy with Eq. (32). Consequently, the magnetic energy stored in the two degrees of freedom [x and y, Eq. (33)] associated with the tipping angle θ is given by the equipartition theorem. Equation (34) implies that a spin temperature T_s exists but does not require that T_s is necessarily equal to T. We note that $\langle\theta\rangle = 0$. The expression for the thermal magnetic energy in Eq. (34) results from the random torque $MH_z\theta$ imposed upon the spin system by random field fluctuations. The torque is identified from the pendulum Langevin equation, obtained from the spin-circuit coupling equation (see Appendix B):

$$\ddot{\theta} + \omega\dot{\theta}/2Q + \pi\gamma\omega\xi M\theta = F(t) .$$

This equation expresses the coupling of a single Bloch vector M to the RLC circuit together with a fluctuating driving noise torque term $F(t)$. The above equation can be recast in the form

$$I_M\ddot{\theta} + \beta\dot{\theta} + MH_z\theta = F'(t) ,$$

where the torque $MH_z\theta$ has been introduced. Here, I_M and β represent respectively the moment of inertia and damping coefficient of the spin pendulum. The equilibrium value of $\langle\theta^2\rangle$ is maintained by the statistical balance of torques due to spin noise radiation emission (which tends to decrease θ), and absorption of noise by the spins (which tends to increase θ).

Except for the extreme nonlinear condition at $T_s = \infty$, we may write Eq. (33) as

$$\langle\theta^2\rangle = \frac{2}{N}\coth^2\left[\frac{\hbar\omega}{2k_BT_s}\right] , \tag{35}$$

which becomes $8(k_BT_s/\hbar\omega)^2/N \ll 1$ in the high temperature limit. It is difficult to violate the condition $\langle\theta^2\rangle \ll 1$ here because $N \approx 10^{22}$. The slightest amount of spin-lattice (T_1) relaxation makes T_s sufficiently small for the condition $(k_BT_s/\hbar\omega)^2 \ll N$ to be obeyed.

Although the spin-pendulum model is phenomenological, it yields quantitative predictions of emitted spin noise power in the limit $R_s/R_i \ll 1$, and accounts for the equipartition of energy when a spin temperature T_s is defined. We may go a step further and estimate from the model the fluctuations in spin population of the spin system coupled to the single-cavity mode. For example, at zero temperature an isolated spin system would have all spins $N = N_\uparrow$ in the ground state. However, if the spins are coupled to the cavity mode the excited state is admixed with the ground state, and the fraction of spins in the excited state is given by

$$f(0) = \langle\sin^2(\theta/2)\rangle \approx \langle\theta^2\rangle/4 .$$

At $T = 0$, Eq. (35) implies that $\langle\theta^2\rangle = 2/N$ and the ensemble of N spins exhibits an average occupation of $Nf = \frac{1}{2}$ spin in the excited state. At any spin temperature T_s the average magnetization along the applied field is given by

$$M_z = M\langle\cos\theta\rangle ,$$

where $M = N\mu\tanh(\hbar\omega/k_BT_s)$. Therefore $M\langle\theta^2\rangle/2$ represents the mean square deviation of M_z from the Boltzmann equilibrium values, as measured along H_0, where

$$\langle\cos\theta\rangle \approx 1 - \langle\theta^2\rangle/2 .$$

This time average implies that the quantization of M is slightly tilted from the H_0 direction because the spin system is coupled to the cavity mode as well as to the field H_0.

VII. SIGNAL-TO-NOISE RATIO

In addition to its fundamental interest, the measurement of nuclear spin noise may have a practical value in situations where T_1 is too long for the application of conventional techniques. It is therefore of interest to determine the conditions under which nuclear spin fluctuations are observable.

If we assume that the resolution bandwidth of the spectrum analyzer is small compared with the linewidth of the spins, the relative mean square uncertainty in the measurement of the spectral density S at a given frequency is given approximately[12] by $\langle\Delta S^2\rangle/S^2 = 1/Bt$, where $\langle\Delta S^2\rangle$ is the mean square uncertainty in the spectral density, B is the resolution bandwidth of the spectrum analyzer, and t is the time over which the measurement is made. We define the signal-to-noise ratio for the measurement of spin fluctuations at a given frequency to be

$$S/N = (S_v^s)^2/\langle\Delta S^2\rangle = [(S_v^s)^2/(S_v)^2]Bt ,$$

where $S_v^s = 4k_BT_sR_s(T_s)$ for spin resistance $R_s(T_s)$ at spin temperature T_s, and S_v is the spectral density of the total effective-noise voltage in the circuit. For $R_s \ll R_i$, $S_v = 4k_B(T + T_N)R_i$, where T_N is the noise temperature of the receiver. Since $R_s(T_s)T_s$ is independent of temperature, we can replace $R_s(T_s)T_s$ in the expression for S_v^s

with $R_s(T)T$ yielding $S_v^s = 4k_B T R_s$, where R_s is evaluated at the bath temperature T. Thus

$$\frac{S}{N} = \left[\frac{R_s T}{R_i(T+T_N)}\right]^2 Bt = \left[\frac{4\pi\xi\chi''Q}{1+T_N/T}\right]^2 Bt \ . \quad (36)$$

For optimum signal-to-noise ratio it is desirable to have the bandwidth B as large as possible. For $B > 1/T_2$, however, the spin noise signal will be smeared out, resulting in a reduction of the signal-to-noise ratio. The optimum bandwidth B is therefore of order $1/T_2$.

We can estimate the expected averaging time for our experiment by inserting appropriate parameters into Eq. (36). The noise temperature T_N for the receiver is about 2 K, and for the data in Fig. 5 we have $B = 300$ Hz, $R_s/R_i \approx 0.1$, and $S_v^s/\Delta S \approx 15$. Under these conditions we find $t = 300$ sec. If the spectrum analyzer is of the scanning type this is the time required to average a range of frequencies equal to one resolution bandwidth B. To average a wider range of frequencies Δf (with the same resolution bandwidth) one must use a time $t_{\Delta f} = t(\Delta f/B) = 2.2$ h for the bandwidth $\Delta f = 8$ kHz used in our experiments. If however, the spectrum analyzer is of the Fourier transform type, t is the total averaging time. This distinction can be understood by realizing that a Fourier transform spectrum analyzer examines all frequencies simultaneously while a scanning spectrum analyzer measures only one frequency at a time.

We now compare the signal-to-noise ratio obtained in the spin noise experiment with that obtained in a conventional (continuous or pulsed) experiment. If we neglect amplifier noise, the signal-to-noise ratio for homogeneously broadened spins in a conventional NMR experiment is given by[13]

$$\frac{S}{N} \approx \frac{\pi\xi Q\omega v_s M_0^2 T_2 t}{k_B T T_1} \ . \quad (37)$$

This expression is derived under the assumption that the magnetization is in equilibrium ($dM_z/dt = 0$) with the applied field H_1. The maximum signal-to-noise ratio occurs when $H_1^2 = 1/\gamma^2 T_1 T_2$ and $M_z = M_0/2$. To compare the signal-to-noise ratio between the spin noise and the conventional NMR experiment we define the quantity

$$\Gamma = \frac{(S/N)_{\text{spin noise}}}{(S/N)_{\text{conventional}}} \ .$$

From Eq. (36) with $T_N = 0$ and $B = 1/T_2$ and Eq. (37) we find that

$$\Gamma \approx A(k_B T/\omega)T_1 = AT_1 n_p \ , \quad (38)$$

where $A = 2\pi Q\hbar\gamma^2/v_c$ is the spontaneous emission rate for the spin radiation into the circuit, and $n_p = k_B T/\hbar\omega$ is the number of photons in the cavity. For T_1 larger than a critical value $T_{1_c} = 1/An_p$, Γ becomes larger than unity and it would become desirable to use the spin noise technique. We can estimate T_{1_c} for our experiment using the values $A = 2\times10^{-16}$ sec^{-1}, $T = 1.5$ K, and $\omega_s = 2\times10^8$ sec^{-1} to find $T_{1_c} = 3\times10^{12}$ sec $= 8\times10^4$ years. This result implies that the spin noise technique would never supplant the conventional technique as a way of performing spin resonance. We note, however, that this derivation assumed that in the conventional method the condition $M_z = M_0/2$ was satisfied from the beginning of the experiment. A more realistic derivation of Γ would assume that in the conventional measurement, M_0 is initially zero and builds up as the measurement is made. However, even with this more realistic assumption, T_{1_c} would be on the order of 1 year for the conditions of our experiment. Thus, although we would not rule out the possibility that the spin noise technique might have an advantage over conventional measurements in certain special cases, in general it seems that spin noise is likely to remain of fundamental interest rather than of practical importance.

VIII. CONCLUDING REMARKS

The very low noise temperature of the dc SQUID as a radiofrequency amplifier has made possible the first observations of spontaneous emission from nuclear spins. A two-level spin system placed in the inductor of a RLC circuit introduces an additional resistance and inductance, defined in terms of nuclear susceptibilities. In accordance with the Nyquist theorem, this additional resistance is accompanied by voltage fluctuations, which are temperature independent for a two-level system. The resonance absorption of Nyquist noise energy from R by the spins is observed as a dip in the noise spectrum of the tuned circuit when the spins are in thermal equilibrium. On the other hand, of greater significance is the bump observed in the noise spectrum when the spins are at infinite spin temperature. An analysis of power flow in this nonequilibrium situation (in which induced absorption and emission cancel) demonstrates that the noise bump is equivalent to spontaneous emission.

The standard solutions to Bloch's equations modified for radiation damping are consistent with the results of the Nyquist theorem for the flow of power from the spins into the circuit. This derivation includes a generalization of previous treatments of radiation damping to cases of arbitrary Q, which should apply to the coherent case as well as to our case of spin noise. Because one measures the total noise from both spins and circuit, direct effects of radiation damping and frequency pulling do not appear in the Nyquist formulation. Using a spin pendulum model, one can show that the populations of the spin states deviate slightly from the Boltzmann distribution. This deviation, which persists down to $T = 0$, occurs because the spin ensemble is coupled to the single cavity mode, and cannot be viewed as an isolated spin system in pure eigenstates.

While the observation of spontaneous emission is made easier by the use of a high-Q circuit at liquid ^{4}He temperatures, in principle it should be observable in any system which displays radiation damping. The concept of spin noise can be extended to many other situations, for example, electron spin resonance and atomic transitions where the emission is enhanced by cavity modes. In the latter case the equivalence of spin noise would be observed as electric dipole noise in the electric field modes of a cavity.[4]

This work was supported by the Director, Office of Energy Research, Office of Basic Energy Sciences, Materials

Sciences Division of the U.S. Department of Energy under Contract No. DE-AC03-76SF00098 (C.H and J.C.) and by the National Science Foundation under Contract No. DMR83-08082 (T.S. and E.L.H.).

APPENDIX A

The expression for any induced reaction field $H_r(t)$ as a convolution integral is derived from the equation for the coupling of spins to the circuit.[10] The coupling constant $k(\omega)$ [Eq. (23)] and the Fourier transform $H_r(\Delta\omega) = -ik(\omega)m(\Delta\omega)$ [Eq. (26)] are then obtained. With $m(t)$ defined according to Eq. (19) and $\Delta\omega_f = 0$, the spin-coupled circuit equation is

$$dH_r(t)/dt + yH_r(t) = -\pi\xi\omega i m(t) , \tag{A1}$$

where $y = \omega/2Q - i\Delta\omega_{sc}$ and $\Delta\omega_{sc} = (LC)^{-1/2} - \omega_s$. Integration of Eq. (A1) results in

$$\begin{aligned} H_r(t) &= -\pi i\omega\xi \int_{-\infty}^{t} e^{y(t'-t)} m(t')dt' \\ &= -\pi i\omega\xi \int_0^{\infty} e^{-y\tau} m(t-\tau)d\tau . \end{aligned} \tag{A2}$$

From Eq. (A2) we define

$$k(\tau) = \sqrt{2\pi}\pi\omega\xi e^{-y\tau} , \tag{A3}$$

and the Fourier transform of $k(\tau)$ is therefore

$$\frac{1}{\sqrt{2\pi}} \int_{-\infty}^{\infty} k(\tau) e^{i\Delta\omega\tau} d\tau = k(\omega)$$

or

$$k(\tau) = \frac{1}{\sqrt{2\pi}} \int_{-\infty}^{\infty} k(\omega) e^{-i\Delta\omega\tau} d\Delta\omega ,$$

where $k(\omega) = 2\pi Q\xi R_i/Z_c$. Thus we express Eq. (A2) in Eq. (14c) as the convolution

$$-ik(t) * m(t) = H_r(t) = \frac{-i}{\sqrt{2\pi}} \int_0^{\infty} k(\tau) m(t-\tau) d\tau , \tag{A4}$$

giving the Fourier transform $H_r(\Delta\omega) = -ik(\omega)m_r(\Delta\omega)$ expressed in Eq. (26).

The low-Q limit $\omega/2Q \ll 1/\tau_r$ does not take into account the effect of the transverse relaxation time T_2. In the absence of T_2, the rate $1/\tau_r$ specifies that the total magnetization M, after having been tipped away from the z axis, remains constant and returns toward the z axis at the precession rate $\dot{\theta} = \gamma H_r = -(1/\tau_r)\sin\theta$ in the frame rotating at $\omega_s = \omega_c$. In Eq. (A1) the low-Q condition is generally expressed by

$$dH_r/dt \ll \omega_s/2Q .$$

This result takes into account T_2 damping also, since H_r depends on $m_r(t)$ which includes contributions from both rates $1/T_2$ and $\dot{\theta}$. In Eq. (A4) we express the low-Q limit by letting

$$H_r(t) = -ik(\Delta\omega_{sc})m(t) ,$$

where $k(\Delta\omega_{sc})$ is time independent (and allows $\Delta\omega_{sc}$ to be nonzero) if the function $m(t-\tau)$ in Eq. (A4) changes slowly compared to the rate at which

$$k(t) = \sqrt{2\pi}\pi\omega\xi \exp[-t(1/\tau_c - i\Delta\omega_{sc})]$$

changes. Here, $\tau_c = 2Q/\omega$ is the circuit-ring down time. Examination of Eq. (21a) (for $H_1 = 0$) shows that $m(t)$ changes in a time T_2'. The low-Q limit is therefore given explicitly by

$$\omega_s/2Q \gg 1/T_2' = 1/T_2 + \gamma k' M_z ,$$

where $1/T_2 \gg \gamma k' M_z = 1/\tau_R$ is the usual condition in which T_2 damping prevents the observation of much longer radiation damping times τ_R.

APPENDIX B

The pendulum equation discussed in Sec. VI is obtained from the form of Eq. (A1) in which the total noise field $H_T(t)$ is determined from the Langevin equation for $\Delta\omega_{sc} = 0$:

$$\dot{H}_T(t) + \frac{\omega}{2Q} H_T(t) = -2\pi i\omega\xi m(t) + S(t) . \tag{B1}$$

The noise term $S(t)$ is assumed to apply to the local magnetization M where $|m(t)| = v = M\theta$ and $u = \Delta\omega = 0$. Thus for weak $H_T(t)$ fields, we have $\theta \ll 1$ and $\theta = \gamma H_T/2$. Equation (B1) becomes, with change of variables,

$$\ddot{\theta} + \frac{\omega\dot{\theta}}{2Q} + \pi\omega\gamma\xi M\theta = F(t) . \tag{B2}$$

Only the properties of $\langle\theta^2\rangle$, deduced from Eq. (B2) which determines the spin temperature T_s [Eqs. (31) and (34)], are independent of relaxation. Therefore it is assumed that $T_1 = T_2 = \infty$.

---

*Present address: AT&T Bell Laboratories, Murray Hill, NJ 07974.

†Present address: Microelectronic and Computer Technology Corporation, 12100 Technology Blvd., Austin, TX 78727.

[1]C. Hilbert and J. Clarke, Appl. Phys. Lett. **43**, 694 (1983); IEEE Trans. Magn. MAG-21, 1029 (1985); J. Low Temp. Phys. 61 (1985); C. Hilbert, J. Clarke, T. Sleator, and E. L. Hahn, Appl. Phys. Lett. **47**, 637 (1985); Bull. Am. Phys. Soc. **30**, 280 (1985).

[2]Tycho Sleator, Erwin L. Hahn, Claude Hilbert, and John Clarke, Phys. Rev. Lett. **55**, 1742 (1985); Bull. Am. Phys. Soc. **30**, 478 (1985).

[3]F. Bloch, Phys. Rev. **70**, 460 (1946).

[4]E. M. Purcell, Phys. Rev. **69**, 681 (1946). For recent work concerning effects of cavity modes on spontaneous emission, see D. Kleppner, Phys. Rev. Lett. **47**, 233 (1981); D. Meschede, H. Walther, and G. Muller, *ibid.* **54**, 551 (1985); S. Haroche and J. M. Raimond, in *Advances in Atomic and Molecular Physics*, edited by B. Bates and B. Bederson (Academic, New York, 1985), Vol. 20, p. 347.

[5]C. P. Slichter, *Principles of Magnetic Resonance*, 2nd ed. (Springer-Verlag, Berlin, 1978), p. 37.

[6]M. Bloom, E. L. Hahn, and B. Herzog, Phys. Rev. **97**, 1699 (1955).

[7]H. B. Callen and T. A. Welton, Phys. Rev. **83**, 34 (1951).

[8]R. V. Pound, Ann. Phys. (N.Y.) **1**, 24 (1957); F. N. H. Robinson, *Noise and Fluctuations* (Clarendon, Oxford, 1974), pp. 167–170.

[9]In situations where $1/T_2 \gg \omega/Q$ with $R_s/R_i \ll 1$, a sharp circuit resonance would appear on top of a flat spin spectrum. In this case the spin noise power P_s given by Eq. (16) would be reduced by the factor $T_2/(T_R + T_2)$ where $T_R = L_p/R_i$.

[10]N. Bloembergen and R. V. Pound, Phys. Rev. **95**, 9 (1954); C. R. Bruce, R. E. Norberg, and G. E. Pake, Phys. Rev. **104**, 419 (1956).

[11]S. Bloom, J. Appl. Phys. **28**, 800 (1957).

[12]J. S. Bendat and A. G. Piersol, *Random Data; Analysis and Measurement Procedures* (Wiley-Interscience, New York, 1971), p. 188.

[13]N. Bloembergen, E. M. Purcell, and R. V. Pound, Phys. Rev. **73**, 679 (1948).